

Distribution of Coronoid Fracture Lines by Specific Patterns of Traumatic Elbow Instability

Jos J. Mellema, MD, Job N. Doornberg, MD, PhD, George S. M. Dyer, MD, David Ring, MD, PhD

Purpose To determine if specific coronoid fractures relate to specific overall traumatic elbow instability injury patterns and to depict any relationship on fracture maps and heat maps.

Methods We collected 110 computed tomography (CT) studies from patients with coronoid fractures. Fracture types and pattern of injury were characterized based on anteroposterior and lateral radiographs, 2- and 3-dimensional CT scans, and intraoperative findings as described in operative reports. Using quantitative 3-dimensional CT techniques we were able to reconstruct the coronoid and reduce fracture fragments. Based on these reconstructions, fracture lines were identified and graphically superimposed onto a standard template in order to create 2-dimensional fracture maps. To further emphasize the fracture maps, the initial diagrams were converted into fracture heat maps following arbitrary units of measure. The Fisher exact test was used to evaluate the association between coronoid fracture types and elbow fracture-dislocation patterns.

Results Forty-seven coronoid fractures were associated with a terrible triad fracture dislocation, 30 with a varus posteromedial rotational injury, 1 with a anterior olecranon fracture dislocation, 22 with a posterior olecranon fracture dislocation, and 7 with a posterior Monteggia injury associated with terrible triad fracture dislocation of the elbow. The association between coronoid fracture types and elbow fracture-dislocation patterns, as shown on 2-dimensional fracture and heat maps, was strongly significant.

Conclusions Our fracture maps and heat maps support the observation that specific patterns of traumatic elbow instability have correspondingly specific coronoid fracture patterns. Knowledge of these patterns is useful for planning management because it directs exposure and fixation and helps identify associated ligament injuries and fractures that might benefit from treatment.

Clinical relevance Two-dimensional fracture and heat mapping techniques may help surgeons to predict the distribution of coronoid fracture lines associated with specific injury patterns. (*J Hand Surg Am.* 2014;■(■):■–■. Copyright © 2014 by the American Society for Surgery of the Hand. All rights reserved.)

Key words Coronoid, fractures, mapping, elbow, injury.

OBSERVATIONS AND STUDIES based on patient care and computed tomography (CT) scans led to an association of specific coronoid fracture patterns with the overall pattern of traumatic

elbow instability.^{1,2} Knowledge of coronoid fracture types and pattern of traumatic elbow instability contributed to a useful guide to treatment.³ Small transverse tip fractures are associated with terrible triad

From the Orthopaedic Hand and Upper Extremity Service, Massachusetts General Hospital; the Department of Orthopaedic Surgery, Brigham and Women's Hospital, Boston, MA; and the Orthotrauma Research Center Amsterdam, Academic Medical Center, Amsterdam, The Netherlands.

Received for publication April 24, 2014; accepted in revised form June 24, 2014.

J.J.M. received a Fulbright grant and VSBFonds grant.

No benefits in any form have been received or will be received related directly or indirectly to the subject of this article.

Corresponding author: David Ring, MD, PhD, Orthopaedic Hand and Upper Extremity Service, Yawkey Center, Suite 2100, Massachusetts General Hospital, 55 Fruit St., Boston, MA 02114; e-mail: dring@partners.org.

0363-5023/14/■-■-0001\$36.00/0
<http://dx.doi.org/10.1016/j.jhsa.2014.06.123>

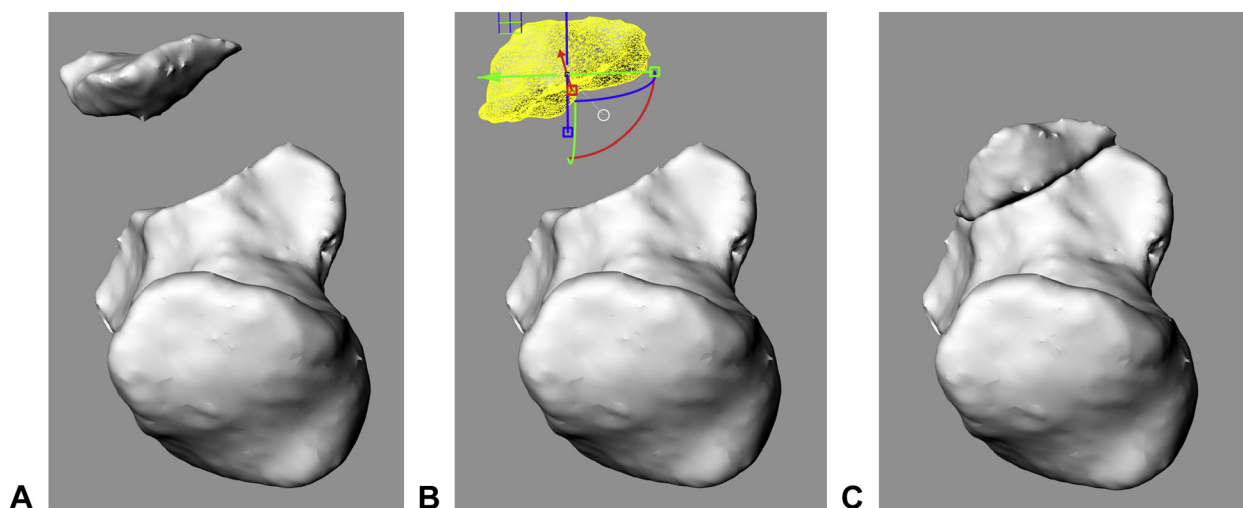


FIGURE 1: Images show fracture fragment reduction of 3-dimensional mesh reconstructions in Rhinoceros (McNeel, Seattle, WA). **A** Imported 3-dimensional mesh reconstruction. **B** Fracture fragment selected for reduction. **C** Image of 3-dimensional mesh reconstruction after reduction of the fracture fragment.

injuries, anteromedial facet fractures with varus postero-medial rotational instability injuries, and larger basal fractures of the coronoid process with anterior and posterior olecranon fracture dislocations.^{4–6}

This study used recently described 2-dimensional fracture mapping techniques in which a map of the most common fracture lines is created by superimposing fracture lines from a large number of injuries^{7,8} after creating quantitative 3-dimensional computed tomography (Q3DCT) models. We also applied heat mapping techniques whereby fracture line intensity is graphically represented in color. These techniques were used to define the location, frequency, distribution, and pattern of fracture lines of the coronoid. We tested the null hypothesis that specific coronoid fractures do not associate with specific overall traumatic elbow instability injury patterns and depicted this on fracture maps and heat maps.

METHODS

Subjects

Our institutional review board approved a retrospective search of our billing data for patients with a coronoid fracture between July 2001 and January 2014 at 2 level I trauma centers. *The International Classification of Disease*, Ninth Revision, *Clinical Modification* (code 813.0x for closed fracture and 813.1x for open fracture) and *Current Procedural Terminology* (codes 24586–24685, including elbow dislocations, Monteggia type of fractures, radial and ulnar fractures) were used to search the billing data. Two hundred seven patients with coronoid fractures were identified. Inclusion criteria were patients aged 18 years or older

with an acute fracture of the coronoid and a CT scan displaying the complete fracture. One hundred twenty-one patients met the inclusion criteria. We excluded 11 patients with prior elbow injury, low-quality CT images, or artifacts on CT scan. Therefore, 110 fractures were available for study.

Two-dimensional fracture mapping

Two-dimensional fracture maps represent fracture line distribution on a 2-dimensional template by superimposing fracture lines from a large number of injuries. Images of coronoid fractures needed for 2-dimensional fracture mapping were based on Q3DCT modeling techniques. The original Digital Imaging and Communications in Medicine files of selected CT scans were obtained through the Picture Archiving Communications System database of the 2 hospitals. All CT scans had a slice thickness between 0.625 mm and 3.000 mm. The digitally imaged files were loaded into 3D Slicer (Boston, MA). The 3D Slicer is a software program used for analysis and visualization of medical images. Bony structures were manually marked on transverse, sagittal, and oblique CT slides using the Paint Effect and additional Threshold Paint option available in this program. After marking all bony structures of the proximal ulna on each CT slide, 3-dimensional polygon mesh reconstructions were created in 3D Slicer. These 3-dimensional mesh reconstructions were imported in Rhinoceros (McNeel, Seattle, WA) for reduction of the fracture fragments (Fig. 1).

Using the method of Cole et al⁸ and Armitage et al,⁷ fracture lines were graphically superimposed onto a

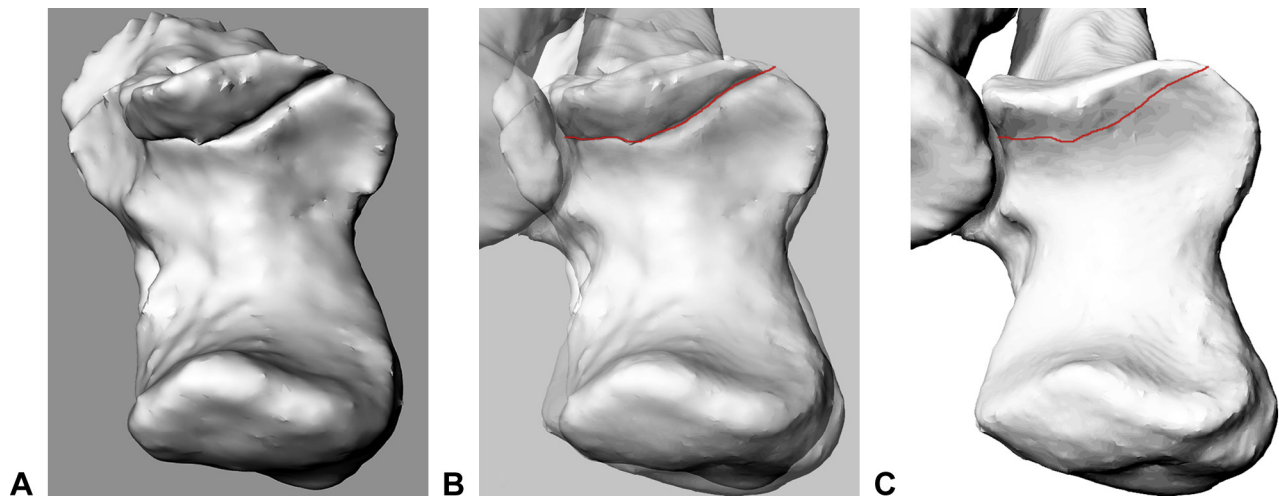


FIGURE 2: Images illustrate the 2-dimensional fracture mapping method. **A** Image of reduced 3-dimensional mesh reconstruction in a similar viewpoint as the template. **B** Fracture line drawn onto superimposed and matched standard 2-dimensional template of an intact proximal ulna. **C** Fracture line drawn onto the template.

2-dimensional template of an intact proximal ulna. Images of the reduced 3-dimensional mesh reconstruction were obtained in the same viewpoint as the 2-dimensional template, imported in Macromedia Fireworks MX software (Macromedia Inc, San Francisco), and matched with the template by aligning anatomical landmarks. After proper alignment of the images with the 2-dimensional template, fracture lines were drawn (Fig. 2).

Heat mapping

To further emphasize the 2-dimensional fracture maps, heat maps were created on which fracture line intensities are graphically represented as colors. The initial diagrams were converted into heat maps with Rhinoceros and Matlab (MathWorks, Natick, MA). All fracture lines were manually and consecutively converted into points (x, y) onto a standard 2-dimensional template of the proximal ulna in Rhinoceros. A standardized space of 0.25 units between points was applied. Subsequently, the point coordinates were exported to Excel (Microsoft Excel, Seattle) and imported in Matlab. Heat maps were created based on these coordinates and by running a data density Matlab script file. Data density is calculated as sum of points, weighted by reciprocal squared distance from the pixel, and shown as heat map.⁹

Patterns of elbow fracture dislocation

Two researchers classified patterns of elbow fracture dislocation based on available anteroposterior and lateral radiographs, 2-dimensional and 3-dimensional

TABLE 1. Demographics (n = 110)

Age (mean ± SD)	46 (16)
Sex, n (%)	
Male	76 (69)
Female	34 (31)
Side of injury, n (%)	
Left	65 (59)
Right	45 (41)
Treatment, n (%)	
Nonsurgically	21 (19)
Surgically	89 (81)
O'Driscoll et al², n (%)	
Type 1	55 (50)
Type 2	29 (26)
Type 3	26 (24)
Injury patterns, n (%)	
Terrible triad	47 (43)
Varus posteromedial rotational instability	30 (27)
Anterior olecranon fracture dislocation	1 (1)
Posterior olecranon fracture dislocation	22 (20)
Posterior Monteggia + terrible triad	7 (6)
Other	3 (3)

CT scans, and intraoperative findings as described in operative reports. Injuries were classified into 1 of the 4 patterns of elbow fracture dislocation described by Doornberg and Ring⁴: the terrible triad elbow fracture dislocation, varus posteromedial rotational instability pattern, anterior or transolecranon fracture dislocation, or posterior olecranon fracture dislocation (type A posterior Monteggia injury according to

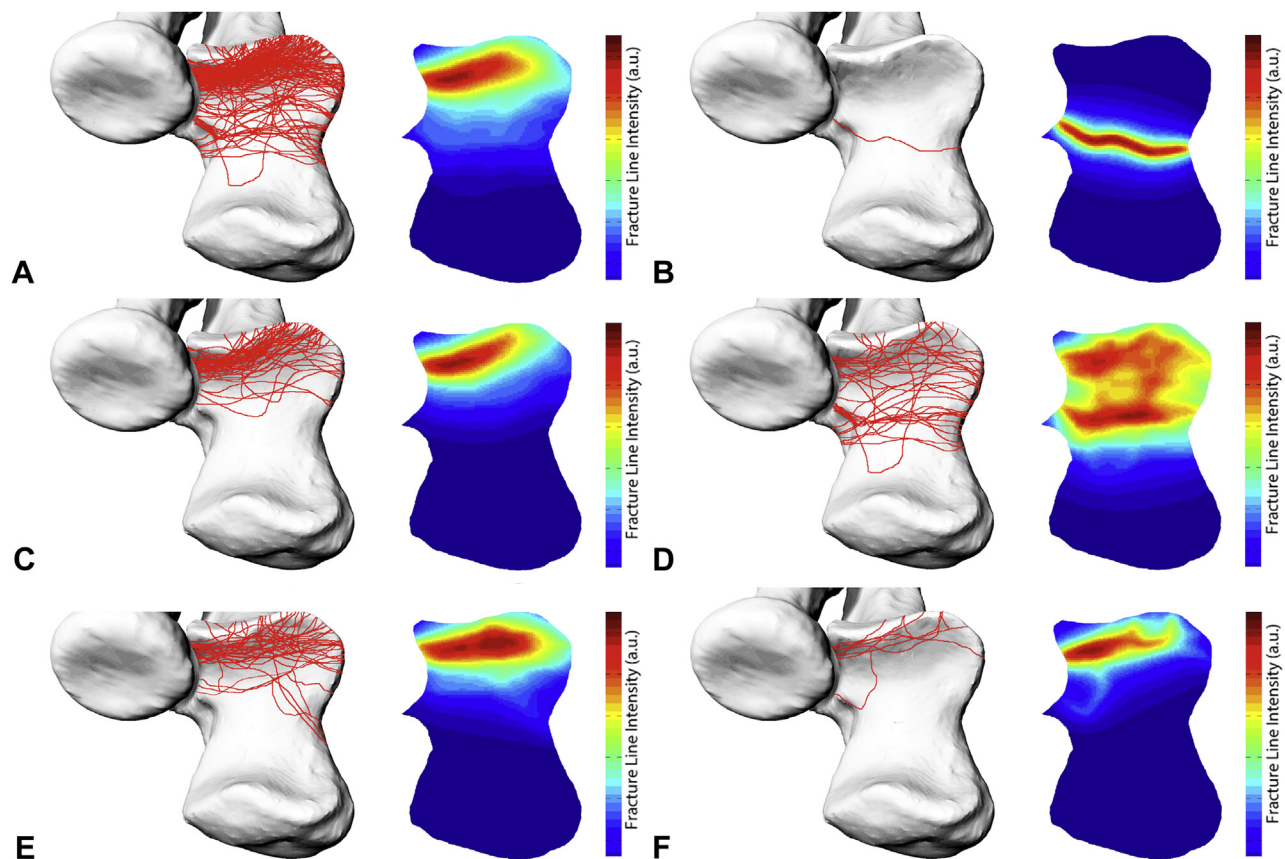


FIGURE 3: Paired fracture and heat maps display patterns and distribution of fracture lines according to specific patterns of traumatic elbow instability. Fracture lines are shown as red lines on the template, and fracture line intensity is illustrated by heat maps following arbitrary units of measure. **A** Overall pattern (n = 110). **B** Anterior olecranon fracture dislocation (n = 1). **C** Terrible triad fracture dislocation of the elbow (n = 47). **D** Posterior olecranon fracture dislocation (n = 22). **E** Varus posteromedial rotational instability pattern (n = 30). **F** Posterior Monteggia injury associated with a terrible triad fracture dislocation of the elbow (n = 7).

the system of Jupiter et al¹⁰). We considered an apex posterior fracture of the proximal ulna combined with complete dislocation of the ulnohumeral joint as a distinct injury pattern.¹¹ This is a variant of the posterior Monteggia lesion, but might be best considered a type of terrible triad injury.¹² In case of disagreement between the researchers, consensus was obtained after discussion.

Classification of coronoid fractures

The classification process was similar for coronoid fractures that were classified according to the system of O'Driscoll et al,² which is also known as the Mayo classification. Type 1 involves fractures of the tip of the coronoid. Type 2 involves a fracture of the anteromedial facet of the coronoid process. Type 3 involves a fracture of the coronoid at the base. In case a fracture type was ambiguous, the type was rated based on the classified elbow fracture dislocation and the most likely associated fracture type.

Statistical analyses

The Fisher exact test was used to evaluate the association between elbow fracture-dislocation patterns and fracture types according to the classification of O'Driscoll et al,² followed by post hoc multiple comparison with Bonferroni correction. Data were analyzed using a standard statistical software package.

RESULTS

There were 76 (69%) men and 34 (31%) women included in this study with an average age of 46 years (range, 18–85 y). The majority of the patients were treated surgically. A total of 55 (50%) patients had a type 1 fracture, and 47 (43%) fractures were associated with a terrible triad fracture dislocation (Table 1).

One patient presented with an isolated, minimally displaced basilar coronoid fracture and was treated nonsurgically. Although this fracture pattern is unusual, this type of fracture was classified as type 3 according to the Mayo classification. Three injuries involved the

TABLE 2. Coronoid Fracture Types and Associated Patterns of Injury

	O'Driscoll et al ²		
	Type 1	Type 2	Type 3
Patterns of Injury			
Terrible triad	42	3	2
Varus posteromedial rotational instability	3	25	2
Anterior olecranon fracture dislocation	0	0	1
Posterior olecranon fracture dislocation	0	1	21
Posterior Monteggia + terrible triad	7	0	0
Other	3	0	0

distal humerus and did not fit into 1 of our injury pattern categories. Two patients had small tip fractures of the coronoid associated with capitellum and trochlea fractures, and one patient had a coronoid tip fracture associated with lateral column humerus fracture.

In 101 (92%) patients, fracture lines entered the proximal radioulnar joint, most commonly at the volar half of the radial notch of the ulna. In terrible triad fracture dislocations, the fracture lines predominantly exited at the tip. In varus posteromedial rotational instability injuries, the fracture lines exited at the anteromedial facet. In the anterior olecranon fracture dislocation, the fracture line entered the proximal radioulnar joint and exited the coronoid at the base. In posterior olecranon fracture dislocations, 9 of 22 (41%) fractures at the base of the coronoid were fragmented, and the most posterior fracture lines exited at the base. In posterior Monteggia injuries with dislocation of the elbow, the fracture lines most often exited at the tip, resembling coronoid fractures associated with terrible triad injuries (Fig. 3).

The association between coronoid fracture types and elbow fracture-dislocation patterns, as shown on 2-dimensional fracture and heat maps, was strongly significant ($P < .001$). Statistically significant associations were found between type 1 fractures and terrible triad fracture dislocations and posterior Monteggia injuries with dislocation of the elbow, between type 2 fractures and varus posteromedial rotational instability injuries, and between type 3 fractures and olecranon fracture dislocations (Table 2).

DISCUSSION

Our fracture maps and heat maps support the observation that specific patterns of traumatic elbow instability

have correspondingly specific coronoid fracture patterns. Moreover, the maps demonstrated fracture patterns similar to coronoid fragment morphology as described by O'Driscoll et al² based on clinical experience. Our data emphasize that determining the pattern of elbow fracture dislocation can be helpful for predicting the type and morphology of coronoid fractures prior to CT imaging and can, therefore, facilitate preoperative planning of surgical approach and fixation techniques.

The strengths of this study are the relatively large number of fractures, Q3DCT modeling techniques that allowed reduction of the fracture fragments and capturing the reduced fracture in the correct viewpoint, and graphic methods to display coronoid fracture line patterns and distribution. There are also several limitations. First, we excluded patients who did not have CT scans. This might have influenced the distribution of elbow injury patterns and associated coronoid fractures because CT scans are more likely to be performed for certain traumatic elbow instability injury patterns. Furthermore, fractures treated without obtaining preoperative CT scans may have important differences from the fractures we studied. Second, the fracture lines were superimposed on a 2-dimensional template. Ideally, we would have used a 3-dimensional template that enabled study from more than one viewpoint. Finally, owing to great anatomical variability of the proximal ulna and especially the coronoid process, some images of the 3-dimensional mesh reconstructions of the coronoid did not match the 2-dimensional template perfectly. Consequently, fracture lines drawn on the 2-dimensional template could slightly differ from true fracture morphology.

Adams et al¹³ felt it was important to distinguish oblique anterolateral and anteromedial fractures of the tip of the coronoid. According to our maps, the tip fractures associated with terrible triad pattern injuries were usually above the sublime tubercle and the anteromedial facet of the coronoid. In other words, they were relatively lateral. Because the anteromedial fractures usually involve a fracture of the coronoid tip, the map was just a bit more medial and actually very similar to that for the tip fractures.

Our findings are consistent with those of Doornberg et al⁴ based on a more qualitative study of radiographs and CT. Our applied techniques verified the strong association of large basilar fractures of the coronoid process with posterior olecranon fracture dislocations, small transverse fractures with terrible triad injuries, and anteromedial facet fractures with varus posteromedial rotational instability injuries. Our study showed that

extra- and intra-articular posterior Monteggia injuries associated with dislocation of the elbow^{11,12} have fractures of the coronoid tip, more akin to terrible triad fracture dislocation of the elbow.

Mapping of fracture lines and the use of heat maps helped verify observed associations for coronoid fractures and specific injury patterns. Knowledge of these patterns is useful for planning management, because it directs exposure, fixation, and identification of associated ligament injuries and fractures that might benefit from treatment. Determining the pattern of traumatic elbow instability may help the surgeon predict the type and morphology of coronoid fracture prior to obtaining a CT study. Given the variability of coronoid fracture patterns, however, determining the elbow injury pattern alone is not sufficient for predicting the type of coronoid fracture precisely. Nevertheless, the strength of the observed associations should facilitate care of patients with limited access to CT imaging. The use of fracture mapping might also be able to determine other useful patterns of injury at other anatomical sites.

REFERENCES

1. O'Driscoll SW. Coronoid fractures. In: Norris TR, ed. *Orthopaedic Knowledge Update: Shoulder and Elbow*. Rosemont, IL: American Academy of Orthopaedic Surgeons, 2002:379–384.
2. O'Driscoll SW, Jupiter JB, Cohen MS, Ring D, McKee MD. Difficult elbow fractures: pearls and pitfalls. *Instr Course Lect*. 2003;52:113–134.
3. McKee RC, McKee MD. Complex fractures of the proximal ulna: the critical importance of the coronoid fragment. *Instr Course Lect*. 2012;61:227–233.
4. Doornberg JN, Ring D. Coronoid fracture patterns. *J Hand Surg Am*. 2006;31(1):45–52.
5. Doornberg JN, Ring DC. Fracture of the anteromedial facet of the coronoid process. *J Bone Joint Surg Am*. 2006;88(10):2216–2224.
6. Doornberg J, Ring D, Jupiter JB. Effective treatment of fracture-dislocations of the olecranon requires a stable trochlear notch. *Clin Orthop Relat Res*. 2004;429:292–300.
7. Armitage BM, Wijdicks CA, Tarkin IS, et al. Mapping of scapular fractures with three-dimensional computed tomography. *J Bone Joint Surg Am*. 2009;91(9):2222–2228.
8. Cole PA, Mehrle RK, Bhandari M, Zlowodzki M. The pilon map: fracture lines and comminution aones in OTA/AO type 43C3 pilon fractures. *J Orthop Trauma*. 2013;27(7):e152–e156.
9. McLean MA, Tirosh I. Opposite GC skews at the 5' and 3' ends of genes in unicellular fungi. *BMC Genomics*. 2011;12:638.
10. Jupiter JB, Leibovic SJ, Ribbans W, Wilk RM. The posterior Monteggia lesion. *J Orthop Trauma*. 1991;5(4):395–402.
11. Strauss EJ, Tejwani NC, Preston CF, Egol KA. The posterior Monteggia lesion with associated ulnohumeral instability. *J Bone Joint Surg Br*. 2006;88(1):84–89.
12. Shore BI, Guitton TG, Ring D. Posterior Monteggia fractures in adults with and without concomitant dislocation of the elbow. *Shoulder Elbow*. 2012;4(3):204–208.
13. Adams JE, Sanchez-Sotelo J, Kallina CF, Morrey BF, Steinmann SP. Fractures of the coronoid: morphology based upon computer tomography scanning. *J Shoulder Elbow Surg*. 2012;21(6):782–788.